

Dynamics of a Josephson fluxon in a long junction with inhomogeneities: theory and experiment

A. A. Golubov, I. L. Serpuchenko,¹⁾ and A. V. Ustinov

Institute of Solid-State Physics, Academy of Sciences of the USSR, Chernogolovka, Moscow Province

(Submitted 23 December 1987)

Zh. Eksp. Teor. Fiz. **94**, 297–311 (June 1988)

Theoretical and experimental investigations are made of a motion of fluxons in long Josephson junctions with a spatially varying distribution of the critical current density. A possibility of resonances between soliton and plasma oscillation modes is predicted and conditions for such resonances are formulated. Numerical calculations of the current-voltage characteristics predict steps corresponding to soliton-plasma resonances. The positions of the steps as a function of the contact parameters are studied. Predicted features are supported by the experimental current-voltage characteristics of Nb-NbO_x-Pb junctions with inhomogeneities introduced deliberately in the insulating spacer. A comparison is made of the experimental results with calculations carried out using perturbation theory and numerical simulation.

1. INTRODUCTION

Nonlinear effects in distributed Josephson junctions are being investigated intensively both theoretically and experimentally. Under weak dissipation conditions, Josephson fluxons (solitons) may exhibit oscillatory motion inside a long junction and be reflected from its edges.^{1,2} Such shuttle motion of fluxons is manifested in the current-voltage characteristic of a junction by steps at multiples of the voltage

$$V_n = n\Phi_0\bar{c}/L, \quad (1)$$

where n is the number of fluxons in a junction, Φ_0 is a magnetic flux quantum, \bar{c} is the Swihart velocity, and L is the length of the junction. In contrast to the Fiske steps,³ which appear in the current-voltage characteristics of short junctions subjected to an external magnetic field, the steps in the characteristics of long junctions at voltages described by Eq. (1) are observed also in the absence of a magnetic field, so that they are usually called zero-field steps.

We shall consider the processes which occur in a long junction with structural inhomogeneities and which have a considerable influence on the current-voltage characteristic. By inhomogeneities in a real Josephson junction we mean the regions inside the junction where there may be variations of the critical current density j_c , the Swihart velocity \bar{c} , the dissipation parameter α , or the distribution of the external current j . Aslamazov and Gurovich⁴ also considered the interaction of solitons with special features in the form of a local magnetic field in the junction. This interaction differs for solitons of opposite signs. Cirillo *et al.*^{5,6} investigated the motion of fluxons in the presence of an inhomogeneity of the form of an inductive region connecting parts of a long junction of finite length. Such a system may exhibit very complex dynamic modes representing sequences of reflections and transmissions of a soliton across an inhomogeneity. The most typical and simplest type of inhomogeneity, which is the one we will consider below, is a region with a local change in j_c . Depending on the sign of the change in j_c such a region represents either a potential barrier ($\Delta j_c > 0$) or potential well ($\Delta j_c < 0$) for a soliton in a junction. In the former case the inhomogeneity is called a microshort and in the latter it is called a microresistance.

Gal'pern and Filippov⁷ investigated static bound states of fluxons that appear at individual structural inhomogeneities. They also demonstrated that in a Josephson junction of finite length a change in the external magnetic field may alter the stability and number of different bound states of fluxon structures at inhomogeneities and this should be manifested experimentally in the dependence of the critical current of such a junction on the magnetic field.⁸

The motion of a soliton in a long Josephson junction with a periodically modulated (as a function of position) value of j_c was investigated using perturbation theory by McLaughlin and Scott,⁹ and Mkrtchyan and Shmidt.¹⁰ It was found that plasma waves, of a frequency which depends on the velocity of a fluxon and on the distance a between inhomogeneities, are emitted in the course of the motion of a fluxon in such a junction with a lattice of inhomogeneities. A calculation of the deceleration length of a soliton because of radiation losses during its motion across a lattice of inhomogeneities was calculated in Ref. 11. However, up to now the calculations have not been continued long enough to obtain an experimentally observed current-voltage junction characteristic. Moreover, as shown below, the most interesting processes in a junction which are manifested experimentally in the current-voltage characteristic may occur when the interaction of a soliton with inhomogeneities is not weak and, consequently, is no longer described by perturbation theory. In this case even a qualitative theoretical description requires numerical modeling. The absence of model calculations is the reason why until now there have been no experimental investigations of the characteristics of long Josephson junctions with inhomogeneities, which would have made it possible to compare the theoretical conclusions with experiments.

Our aim was to investigate theoretically and experimentally the dynamics of a soliton and the current-voltage characteristic of a long Josephson junction with periodic inhomogeneities of the critical current density.

The paper is organized as follows. The investigated model of a junction with periodic inhomogeneities is formulated in Sec. 2. The solution of the problem obtained using perturbation theory is given in Sec. 3 and the radiation field

of a moving fluxon is calculated there. The conditions under which a soliton can interact resonantly with plasma waves are formulated. This interaction is analyzed in detail by numerical methods in Sec. 4, where the current-voltage characteristic of the junction is calculated and an analysis of the resultant singularities is made. The results of an experimental investigation of tunnel junctions with deliberately induced periodic inhomogeneities are reported and compared with the theory in Sec. 5.

2. MODEL OF A JUNCTION

According to the one-dimensional model of a Josephson junction, the difference between the phases of the order parameter of electrons $\varphi(x, t)$ obeys a modified sine-Gordon equation⁹:

$$\varphi_{xx} - \varphi_{tt} = f(x) \sin \varphi + \alpha \varphi_t + \gamma, \quad (2)$$

where the spatial coordinate x is normalized to the Josephson penetration depth $\lambda_J = (2e\mu_0\Lambda j_{c0}/\hbar)^{-1/2}$; the time t is normalized to the reciprocal of the plasma frequency $\omega_p^{-1} = (C\hbar/2ej_{c0})^{1/2}$, where j_{c0} is the average critical current density per unit length of the junction; $\Lambda = \lambda_1 + \lambda_2 + d$ is the magnetic thickness of the junction barrier; d is the thickness of the insulating spacer; λ_1 and λ_2 are the depths of penetration of the magnetic field into the superconducting films; $C = \epsilon\epsilon_0 W/d$ is the capacitance of the junction per unit length; W is the width of the junction in the direction perpendicular to the x axis. The function $f(x) = j_c(x)/j_{c0}$ gives the distribution of the critical current density along the junction, whereas the coefficient $\alpha = G(\hbar/2ej_{c0}C)^{1/2}$ is related to the dissipation of energy in the junction and is proportional to the quasiparticle conductance G per unit length. The last term in Eq. (2) $\gamma = j/j_{c0}$ represents a uniformly distributed external current j assumed to be independent of x . A uniform distribution of j along the junction is possible in the first approximation only for a junction with a transverse geometry of length $L \gg \lambda_J$ in the x direction and width $W \lesssim \lambda_J$.¹²

If a Josephson junction is not closed to form a ring, Eq. (2) should be supplemented by the boundary conditions at the edges of the junction:

$$\varphi_x(0) = \varphi_x(l) = h, \quad (3)$$

where h is the external magnetic field normalized to

$$\Phi_0/2\pi\Lambda\lambda_J, \quad l = L/\lambda_J.$$

In the case of a ring junction geometry the boundary conditions corresponding to one fluxon pinned in a junction are of the form¹³

$$\varphi(0, t) = \varphi(2\pi r, t) + 2\pi, \quad \varphi_x(0, t) = \varphi_x(2\pi r, t), \quad (4)$$

where r is the junction radius.

We shall assume that the inhomogeneities are localized in comparison with λ_J . Then, if a junction contains a finite number N of inhomogeneities of the insulating barriers separated by equal distances, they can be modeled by the function⁹

$$f(x) = 1 + f_0 \sum_{n=1}^N \delta(x - an), \quad |f_0| \ll 1. \quad (5)$$

The sign of the coefficient f_0 in front of the δ function determines the type of inhomogeneities: $f_0 < 0$ corresponds to microresistances attracting a soliton, and $f_0 > 0$ corresponds to microshorts repelling it.

3. PERTURBATION THEORY

We can calculate the field of the radiation emitted by a fluxon traveling in an infinitely long junction when $\alpha \neq 0$ and $f(x)$ is in the form of Eq. (5) ($N = \infty$) if we use perturbation theory developed in Refs. 9 and 10. We shall seek the solution of Eqs. (2) and (5) in the form

$$\varphi(x, t) = \varphi_0(x, t) + \varphi_1(x, t), \quad \varphi_1 \ll \varphi_0, \quad (6a)$$

where

$$\varphi_0(x, t) = \arctg \left[\exp \left(\frac{x - \beta t}{\nu} \right) \right], \quad (6b)$$

and $\nu = (1 - \beta^2)^{1/2}$ is a one-soliton solution of this equation for $f_0 = 0$. The soliton velocity β determined from the condition of energy balance between the external force γ and the dissipation α , is given by⁹

$$\beta \approx \left[1 + \left(\frac{4\alpha}{\pi\gamma} \right)^2 \right]^{-1/2}, \quad \alpha \ll \gamma. \quad (7)$$

Substituting Eqs. (6a) and (6b) into Eq. (2), we obtain a linear differential equation for the function $\varphi_1(x, t)$ which determines the radiation field of a fluxon:

$$\left(\frac{\partial^2}{\partial x^2} - \frac{\partial^2}{\partial t^2} - \alpha \frac{\partial}{\partial t} - \cos \varphi_0 \right) \varphi_1 = f_0 \sin \varphi_0 \sum_{n=-\infty}^{+\infty} \delta(x - an). \quad (8)$$

The solution of Eq. (8) in a coordinate system linked to a moving soliton

$$\xi = \frac{x - \beta t}{\nu}, \quad \tau = \frac{t - \beta x}{\nu}, \quad (9)$$

can be represented in the form

$$\begin{aligned} \varphi_1(\xi, \tau) = & -f_0 \sum_{n=0}^{\infty} \operatorname{Re} \left\{ \exp(-i\omega_n \tau) \right. \\ & \left. \times \int_{-\infty}^{+\infty} G(\omega_n, \xi, \xi') \sin \varphi_0(\xi') \exp(-ik_n \xi') d\xi' \right\}, \end{aligned} \quad (10)$$

where $\omega_n = un\beta/\nu$; $k_n = un/\nu$; $u = 2\pi/a$; G is the Green's function of the differential operator on the left-hand side of Eq. (8), known from Ref. 14 and equal to

$$\begin{aligned} G(\omega_n, \xi, \xi') = & \\ = & - \frac{\exp\{-\alpha\beta(\xi - \xi')/2\nu - Q_n|\xi - \xi'|\} (\operatorname{th} \xi \pm Q_n) (\operatorname{th} \xi' \mp Q_n)}{Q_n(1 \pm Q_n)}, \end{aligned} \quad (11)$$

where

$$Q_n = (1 - \omega_n^2 - i\alpha\omega_n/\nu)^{1/2}, \quad |\omega_n| \ll 1, \quad (12a)$$

$$Q_n = -i(\omega_n^2 - 1 + i\alpha\omega_n/\nu)^{1/2}, \quad \omega_n > 1. \quad (12b)$$

Substituting Eqs. (11) and (12) into Eq. (10) and integrating, we obtain the following expression for the radiation field far from a soliton (i.e., when $|\xi| \gg 1$):

$$\varphi_1(\xi, \tau) = -\frac{\pi}{4} f_0 \sum_{n=0}^{\infty} \operatorname{Re} \left\{ \frac{b_n^2 + (6 \mp 2Q_n) b_n + 11 \pm 4Q_n}{Q_n(1 \mp Q_n) \operatorname{sh}(\pi b_n/2)} \right. \\ \left. \times \exp(-i\omega_n \tau - \delta_n \xi) \right\}, \quad (13)$$

where $\delta_n = (\alpha\beta/2v) \pm Q_n$ and $b_n = -ik_n + \delta_n$. The upper signs in Eqs. (11) and (13) correspond to $\xi \gg 1$, i.e., to the emission of φ_1^+ ahead of a fluxon, whereas the lower signs correspond to $\xi \ll -1$, i.e., to the emission of φ_1^- behind a fluxon.

Adopting a system of coordinates at rest (x, t) , we can write down Eq. (13) in the form of a superposition of oscillations traveling in a junction

$$\varphi_1(x, t) = \sum_n A_n \exp[i(\omega_{pi}t - k_{pi}x)], \quad (14)$$

which obey the plasma dispersion law

$$\omega_{pi}^2 = 1 + k_{pi}^2, \quad (15a)$$

where

$$\omega_{pi}(\beta) = \frac{un\beta}{v^2} \pm \frac{\beta}{v} \left(\frac{u^2\beta^2 n^2}{v^2} - 1 \right)^{1/2}, \quad (15b)$$

$$k_{pi}(\beta) = \frac{un\beta^2}{v^2} \pm \frac{1}{v} \left(\frac{u^2\beta^2 n^2}{v^2} - 1 \right)^{1/2}. \quad (15c)$$

The expressions represented by Eqs. (15b) and (15c) reduce for $n = 1$ to those obtained earlier in Ref. 10 in the case when $\alpha = \gamma = 0$ and the critical current density $j_c(x)$ is subject to sinusoidal modulation.

According to Eq. (13), the amplitudes A_n of plasma oscillations in Eq. (14) decrease exponentially as n increases for $un \gg 1$, so that the sum over n is dominated only by the terms for which we have $un \approx 1$. In the most typical case of $u \approx 1$, which will be discussed below (i.e., when the period $a\lambda_j = 2\pi\lambda_j/u$ of lattice inhomogeneities is of the order of the Josephson length λ_j) the sum is determined by the term $n = 1$, i.e., by the first Fourier harmonic of the function $f(x)$. However, we can easily show that the term with $n = 0$ in Eq. (13) vanishes for $|\xi| \gg 1$, i.e., the constant component of the function $f(x)$ makes no contribution to the radiation.

It also follows from Eq. (13) that the radiation energy losses S experienced by a fluxon are proportional to the electric φ_{1z} and magnetic φ_{1x} fields, and depend nonmonotonically on the soliton velocity β (Ref. 10). The losses are maximal when $\beta = \beta_t = (1 + u^2)^{-1/2}$ and then as β increases the value of S vanishes when $\beta_0 = 1/u$ (provided $u > 1$). In the interval $\beta_0 < \beta < 1$ the function $S(\beta)$ has a smooth maximum and in the limit $\beta \rightarrow 1$, because $\varphi_1(x, t) \rightarrow 0$, we have $S \rightarrow 0$. Here, β_t denotes the threshold velocity of a soliton such that for $\beta < \beta_t$ the radiation is not propagated in a junction, but is localized near a vortex in a region of dimensions of the order of $[1 - u^2\beta^2/(1 - \beta^2)]^{-1/2}$ [the quantities ω_{pi} and k_{pi} in Eq. (15) are then complex]. For $\beta > \beta_t$ and $\alpha = 0$, a wave travels in a junction, but for $\alpha \neq 0$, it decays in a distance l_α , which in a system of coordinates at rest (x, t) is

$$l_\alpha = v/(u\alpha)^{1/2}, \quad \beta \gg \beta_t, \quad (16a)$$

$$l_\alpha = 2v/\alpha, \quad \beta \approx 1. \quad (16b)$$

Using the system (15) we can readily show that β_0 is equal to the soliton velocity at which the group velocity of the

radiation behind it is $v_g = d\omega_{pi}(\beta)/dk_{pi}(\beta) = 0$. We shall ignore here the radiation ahead of a fluxon φ_1^+ (when $\xi + \infty$) because it follows from Eq. (13) that in the interval $\beta_t < \beta < 1$ the inequality $|\varphi_1^-| \gg |\varphi_1^+|$ is obeyed (with the exception of the region where $\beta \approx \beta_t$).¹⁰

Therefore, an analysis carried out using perturbation theory shows that a fluxon moving in an inhomogeneous infinitely long junction emits plasma waves the decay (damping) length of which is governed by the dissipation α and by the fluxon velocity β . The expressions obtained for the radiation field make it possible to calculate, in principle, the relevant losses and the corrections to the current-voltage characteristic of a contact. However, in the case of a real Josephson junction of finite length we can assume also a different mechanism of energy losses by a soliton, which involves transfer of energy to plasma oscillations. In a ring junction of radius r the frequency of a soliton oscillation mode is given by

$$\omega_{sol} = 2\pi\beta/2\pi r = \beta/r. \quad (17)$$

Oscillations of frequency ω_{sol} can interact in a junction with plasma oscillations of frequency ω_{pi} given by Eq. (15). The condition for the appearance of resonances between these two oscillation modes can be written as follows:

$$m\omega_{sol} = m'\omega_{pi}, \quad (18)$$

where m and m' are integers.

Bearing in mind that in the case of a sufficiently long junction we have $\omega_{sol} \ll \omega_{pi}$, we shall consider mainly the case when $m' = 1$. The opposite case $m' > 1$ corresponds to resonances implying the interaction of a soliton with a plasma mode after the soliton repeatedly goes back and forth in the junction, during which process the plasma oscillations decay if the dissipation α is not too small. If $m' = 1$, Eq. (18) becomes

$$m\omega_{sol} = \omega_{pi}. \quad (19)$$

Substituting in Eq. (19) the expression for ω_{pi} from Eq. (15b), and then using Eq. (17), we obtain an expression for the fluxon velocity β_m at which resonances may appear:

$$\beta = \left[\left(1 - \frac{2\pi r}{ma} \right) + \frac{r}{m} \right], \quad (20a)$$

$$m < \frac{2\pi r}{a} (1 - \beta_m^2)^{-1}, \quad \beta_m < 1. \quad (20b)$$

Near resonances $\beta \sim \beta_m$ the amplitude of a plasma oscillation mode should increase and then the perturbation theory approximation corresponding to $|\varphi_1| \ll |\varphi_0|$ becomes invalid. Therefore, perturbation theory can be used to estimate only the positions of resonances β_m in accordance with Eq. (20). In studies of resonance profiles we have to use other methods.

4. NUMERICAL MODELING

The influence of soliton-plasma resonances on the current-voltage characteristic of a ring junction with regularly distributed inhomogeneities was investigated by solving numerically the sine-Gordon equation (2). The function $f(x)$ was written in the form

$$f(x) = 1 + \operatorname{sign}(f_0) \sum_{n=1}^N \left\{ 1 - \operatorname{th}^2 \left[\frac{2}{f_0} (x - an) \right] \right\}. \quad (21)$$

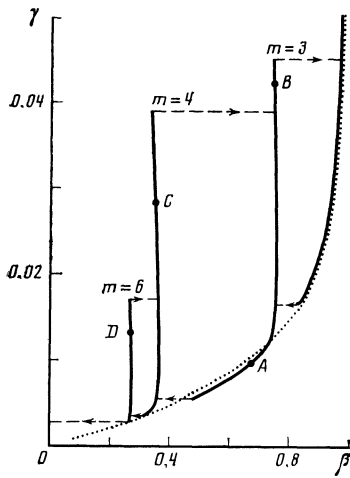


FIG. 1. Current-voltage characteristic in the region of the first zero-field step calculated for homogeneous (dotted curve) and inhomogeneous (continuous curves) ring Josephson junctions. The values of the parameters are given in the text.

A stabilized explicit difference scheme was used in this numerical modeling.¹⁵ The steps along x and t were 0.05. The accuracy was controlled by halving and doubling the step. The continuous curves in Fig. 1 represent the numerically calculated part of the current-voltage characteristic in the region of the first zero-field step (i.e., the soliton velocity as a function of the external current γ) for a ring junction with the following parameters: $2\pi r = 10$, $\alpha = 0.01$, $N = 5$, $a = 2$, $f_0 = -0.4$. The dotted curve in the same figure represents the current-voltage characteristic of a homogeneous junction calculated by the same method by substituting $f(x) = 1$ in Eq. (2), but assuming the same values of the parameters r and α as before. We can see that the two calculated current-voltage characteristics are quite different. The characteristic of a junction with inhomogeneities has additional steps at almost fixed voltages and, as identified by arrows in Fig. 1, hysteresis is observed. If we move along one of the branches of the current-voltage characteristic in the direction of decreasing current γ , then at some value $\gamma = \gamma_l$ the voltage decreases abruptly and a transition takes place to a different branch. As we move along this branch, an upward

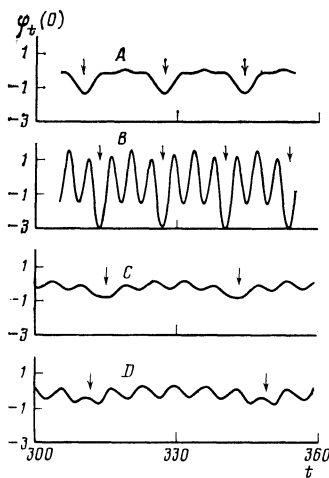


FIG. 2. Dependences of the numerically calculated voltage $\varphi_v(0, t)$ on time t . Curves A , B , C , and D correspond to the points A , B , C , and D in the current-voltage characteristic shown in Fig. 1. The arrows identify the times at which a soliton passes the point $x = 0$.

abrupt transition to the initial branch occurs at $\gamma = \gamma_u > \gamma_l$.

The reasons for the appearance of these discontinuities in the current-voltage characteristic of a junction with inhomogeneities were identified by investigating the time dependence of the voltage $\varphi_v(x_0, t)$ calculated at a fixed point of the junction and shown for the point $x_0 = 0$ in Fig. 2. The characteristics A , B , C , and D correspond to the points A , B , C , and D of the calculated current-voltage characteristics shown in Fig. 1. The arrows in Fig. 2 identify when a soliton undergoing cyclic motion in the junction passes. We can see from this figure that in the case of an inhomogeneous junction there are oscillations of φ_v with time at a frequency which is an exact multiple of the soliton reversal frequency. Therefore, the condition for a soliton-plasma resonance of Eq. (19), considered in the preceding section, is satisfied. The branches with the points B , C , and D correspond to $m = 3, 4$, and 6 .

It is clear from curve A in Fig. 2 that at the point A on the current-voltage characteristic the amplitude of the plasma oscillations is small. In this region the current-voltage characteristic of a junction with inhomogeneities differs little from the characteristic of a homogeneous junction. The amplitude of plasma oscillations increases with the voltage across the junction as the resonance branch with $m = 3$ is approached. A further increase of the current γ across the junction does not increase the average fluxon velocity and the energy goes into increasing further the amplitude of plasma oscillations without contributing to the average voltage across the junction. Perturbation theory is invalid in this part of the current-voltage characteristic. In the part of the characteristic where the amplitude of plasma oscillations approaches the amplitude of a soliton mode, an instability appears at some point and a transition takes place to a different branch of the current-voltage characteristic located at higher voltages.

The calculated current-voltage characteristic is valid in the range of junction parameters with a small dissipation α satisfying the condition $\alpha l \ll 1$. An increase in α reduces the height of the steps and hysteresis disappears for $\alpha \approx 0.06-0.08$. Then, the theory predicts that the positions of the calculated voltage discontinuities should be practically unaffected. Moreover, it follows from the calculations that an increase in the parameter f_0 from 0.1 to 0.4 also has little effect on the step positions.

We shall now compare the results of this numerical calculation with Eq. (19) obtained in the perturbation theory approximation. Figure 3 shows the positions of the steps corresponding to soliton-plasma resonances in the current-voltage characteristics of ring junctions of length $2\pi r = 10$ and with different numbers of inhomogeneities. The triangles in this figure represent the perturbation theory results of Eq. (20) and the circles are the positions of the steps found by numerical calculation of the current-voltage characteristics on the assumption that $f_0 = -0.4$ and $\alpha = 0.01$. The integers in Fig. 3 are the resonance numbers m .

It is clear from Fig. 3 that Eq. (20) is in quantitative agreement with the results of numerical calculations of the positions of steps on the current-voltage characteristic. The discrepancies are of order 10–20% and they depend on the values of α and m . The numerically calculated steps corresponding to given values of m are located at lower voltages than those calculated from Eq. (20). We may assume that

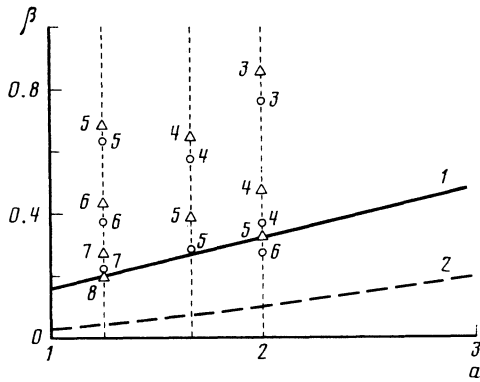


FIG. 3. Comparison of the positions of the steps of the current-voltage characteristics due to soliton-plasma resonances in the case of a ring junction of length $l = 10$ plotted as a function of the period a of a lattice of inhomogeneities: Δ) results calculated using Eq. (20); \circ) results of a numerical analysis; 1) $\beta = \beta_0(a)$; 2) $\beta = \beta_1(a)$.

this difference is associated with the deviations of the plasma wave frequency from that given by Eq. (15) when the radiation amplitude is high and also due to deceleration of a soliton under the action of radiation, which can be included in the next order of perturbation theory. It should also be mentioned that in the case of the numerically calculated current-voltage characteristic shown in Fig. 1 there is no resonance with the number $m = 5$ (see also the points at $a = 2.0$ in Fig. 3). This may be due to the fact that the postulated position of the resonance with $m = 5$ lies in a region where $\beta \approx \beta_0$. In this region the energy transferred by radiation is close to zero, so that the amplitude of the resonance is also small. Therefore, there is a good agreement between the exact numerical results and the simple estimates obtained using perturbation theory.

The results reported above apply to the case of a ring junction in which there is no reflection of a fluxon from the edges. In a linear junction the edges also act as inhomogeneities and this complicates the picture. Numerical calculations for a linear junction carried out by the method described above demonstrate that the fine structure of the current-voltage characteristics is retained.¹⁶ This case is discussed in greater detail in Sec. 6 below where the experimental results are compared with the calculations.

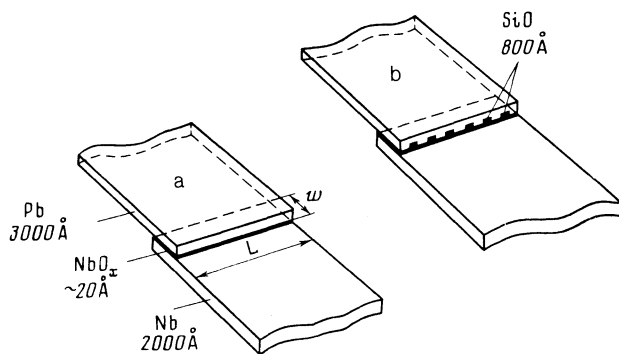


FIG. 4. Schematic diagram showing the experimentally investigated homogeneous (a) and inhomogeneous (b) Josephson junctions with the transverse geometry ($w \ll \lambda_j \ll L$).

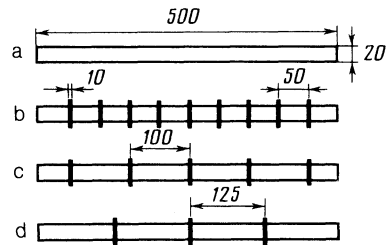


FIG. 5. Configuration of deliberately formed inhomogeneities in the investigated junctions (all the dimensions are in microns).

5. EXPERIMENTS

The effect of a resonant interaction of a soliton with plasma modes was investigated experimentally in Nb-NbO_x-Pb tunnel junctions with deliberately introduced inhomogeneities in the insulating barrier spacer. The junctions were made employing the conventional thin-film technology in which niobium was oxidized in a glow-discharge plasma.¹⁷ Photolithography was used to form 12 junctions with the transverse geometry (of the overlap type) and with $500 \times 20 \mu\text{m}$ dimensions on a silicon substrate of $15 \times 24 \text{ mm}$ size (Fig. 4). Inhomogeneities were produced by explosive photolithography in the form of strips of silicon monoxide oriented across the junctions. The width of the inhomogeneities along a junction was $10 \mu\text{m}$ and their thickness was $\sim 80 \text{ nm}$. Four junctions on the substrate had no inhomogeneities and acted as controls, whereas in the others there were 3, 5, or 9 equidistant inhomogeneities (Fig. 5). Very stringent requirements had to be satisfied during measurements in order to protect a sample from external sources of strays and noise. Measurements were made in a screened cryostat where the residual magnetic field was $\sim 10^{-4} \text{ G}$. A current was set using a stable mercury-zinc device, whereas current and potential contacts were formed by two screened twisted pairs of wires 0.2 mm in diameter for each of the junctions. The sensitivity of the dc measurements was limited by the induced thermo-emf in the measuring wires and in the contacts; this emf was of the order of $0.5 \mu\text{V}$. When the fine-structure branches of the current-voltage characteristics were investigated, this sensitivity could be increased further by a factor of 2-3 by accumulating and averaging the measurements.

The experimental results discussed below were obtained by investigating a substrate with junctions labeled with the batch number 49. We prepared six substrates for junctions with inhomogeneities and only in the case of the last of them were we able to produce junctions with the parameters needed for a comparison between theory and experiment.

We investigated experimentally the profiles of the first zero-steps of the current-voltage characteristic corresponding to the motion of one soliton in each junction. The voltage corresponding to these steps was $V_s \approx 27 \mu\text{V}$ at $T = 4.2 \text{ K}$ and did not vary from junction to junction by more than 2-3%. The parameters of the investigated junctions are listed in Table I.

Figure 6 shows the general appearance of the current-voltage characteristic of a homogeneous control junction No. 49.13 obtained at low voltages. It is known^{1,2} that the number of steps observed in the current-voltage characteris-

TABLE I. Parameters of investigated Nb–NbO_x–Pb Josephson junctions at $T = 4.2$ K.

No. of junction	N_i number of inhomogeneities	j_c , A/cm ²	V_s , μ V	v^*/V_s	l_{exp}	α_{exp}	$l_0 _{exp}$
49.3	5	78	27.0	0.89	12.5	0.010	0.25
49.7	–	81	26.8	–	12.7	0.010	–
49.12	9	89	28.2	0.85	13.3	0.009	0.27
49.13	–	93	27.2	–	13.6	0.009	–
49.14 *	3	60	26.8	0.79	10.8	0.011	0.22

*The characteristics of the junction No. 49.14 were determined after a cycle of heating and cooling of the substrate in the temperature range 4.2–300 K. This was the reason for the somewhat lower value of j_c for this junction compared with other junctions for which the parameters are given in the above table.

tic in zero external magnetic field should be approximately equal to the length of the junction in dimensionless units $l = L/\lambda_J$. It is clear from Table I that in our case such an estimate agrees with the experimental results: the current-voltage characteristic of junction No. 49.13 has 11 zero-field steps (Fig. 6) and an estimate of l_{exp} from the experimental parameters gives ≈ 13.6 . A calculation of j_c from the experimental data was made using a current jump ΔI_g near a gap singularity in the current-voltage characteristic at a voltage of ≈ 3 mV: $j_c \approx 0.7\Delta I_g/S$ (Ref. 2), where S is the junction area. The magnetic thickness of the barrier was calculated allowing for the Swihart velocity \bar{c} deduced from the voltage V_s and amounting for these junctions to about 1/45 of the velocity of light in vacuum. The dissipation factor α was deduced from the slope of the lower part of the first zero-field step.²

Figure 7 demonstrates the main experimental result of the present investigation: we determined the first steps of the current-voltage characteristics of Nb–NbO_x–Pb junctions. In the case of junctions with deliberately formed inhomogeneities we found additional branches in the current-voltage characteristic at voltages V^* lower than the voltage of the first zero-step V_s and which had profiles and positions along the voltage axis that depended on the parameters of the junction and on the number of inhomogeneities in the junction.¹⁸ These features were not exhibited by the current-voltage characteristics of homogeneous junctions.

The fine-structure branches of the current-voltage characteristic exhibited hysteresis which decreased and dis-

appeared on increase in temperature (Fig. 8). The temperature dependences of l_{exp} and α_{exp} were also determined (Fig. 9). Aging of the samples after several cooling and heating cycles in the range 4.2–300 K altered not only the critical current density j_c , but also the positions of the fine-structure branches.

The current-voltage characteristics of the homogeneous junctions labeled Nos. 49.3 and 49.14 had two stable reproducible values of the critical current (Fig. 7). The lower of these values I_{pin} was assumed to be due to pinning of a soliton at one of the inhomogeneities in the junction. An increase in the distance between the inhomogeneities (Figs. 7b–7d) increased I_{pin} , which corresponded to an increase in the pinning force. At $I = I_{pin}$ the current-voltage characteristic exhibited a jump from a steady state in the first zero-field step, which corresponded to unpinning of a fluxon from an inhomogeneity and the onset of its motion along the junction.

6. DISCUSSION OF RESULTS

We shall now compare the results of the theory with the experimental positions of the fine-structure steps in the current-voltage characteristics. In the case of junctions with a transverse geometry and inhomogeneities of the kind used in our experiments, Eq. (20a) is modified to

$$V_m = \left[\left(1 - \frac{2l}{ma} \right)^2 + \left(\frac{l}{\pi m} \right)^2 \right]^{1/2} V_s. \quad (22)$$

The above expression allows for the fact that the spatial period of the revolution of a soliton in the presence of reflections from the junction boundaries is $2l$. We shall ignore the phase shift of soliton oscillations associated with reflection of a soliton into an antisoliton and vice versa. If $l \gg 1$, the time delay due to such a phase shift is small compared with the time period of the soliton revolution.

We can use Eq. (22) to estimate the order of soliton-plasma resonances which appear in a real experimental situation. In the case of deliberately formed inhomogeneities with a known distance between them the calculated positions of the resonances are governed by the Josephson depth of penetration λ_J found from the experimental results (Table I). A comparison of the experimental values of V^* with those calculated on the basis of Eq. (22) made it possible to estimate the order of the observed resonances, which gave $m \approx 11, 6,$ and 5 for the current-voltage characteristics in

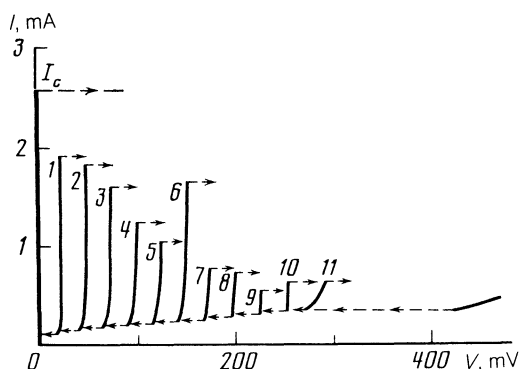


FIG. 6. Zero-field steps in the current-voltage characteristic of a homogeneous Nb–NbO_x–Pb junction No. 49.13 at $T = 5.1$ K.

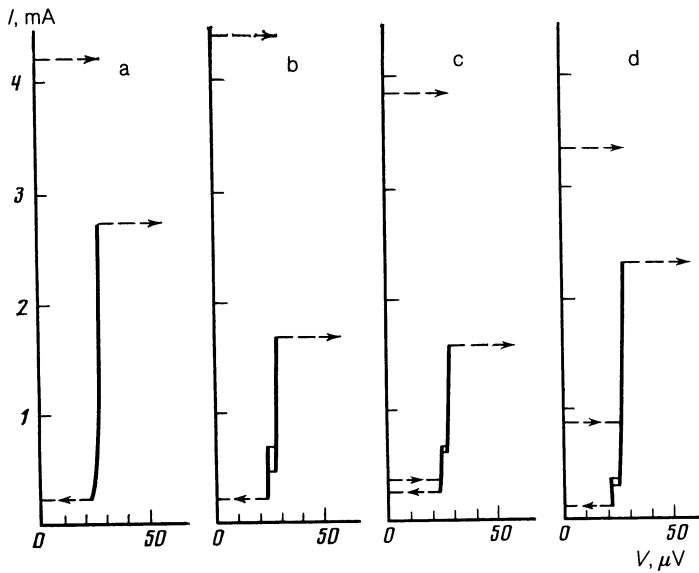


FIG. 7. First zero-field step on the current-voltage characteristic of the investigated Nb-NbO_x-Pb junctions: a) No. 49.13 (homogeneous junction); b) No. 49.12 (nine inhomogeneities); c) No. 49.3 (five inhomogeneities); d) No. 49.14 (three inhomogeneities); $T = 4.2$ K.

Figs. 7b, 7c, and 7d, respectively. In all these characteristics there was only one fine-structure branch. We assumed that this was due to the fact that the other branches were not observed at lower voltages because of a strong instability of the lower parts of the current-voltage characteristics in the presence of external noise and strays during measurements. The range of voltages V in which it was possible to observe the first zero-field steps was at most $0.8V_s \leq V \leq 1.0V_s$, which was true also of control homogeneous junctions. In the case of junction No. 49.3 we deduced from Eq. (22) that there were resonances with numbers $m \geq 6$, where $V_6 \approx 0.85V_s$, $V_7 \approx 0.63V_s$, and $V_8 \approx 0.47V_s$. The experimental value of the voltage for the additional branch was close to V_6 and amounted to $V^* \approx 0.89V_s$. Therefore, under our experimental conditions the calculated branches for junction No. 49.3 with $m \geq 7$ should be outside the investigated part of the current-voltage characteristic. The discrepancy between the results obtained by perturbation theory and the experimental data in the cases illustrated in Figs. 7b-7d was at most 5-8% at the above values of m .

In a detailed comparison of the theory and experiment it was interesting to follow the shifts of the fine-structure branches in the current-voltage characteristics when the distance between the inhomogeneities (expressed in units of λ_J) was altered. In the experiments this could be done by altering the temperature. However, we can see from Fig. 9 that an increase in λ_J with temperature was accompanied by a strong rise of the dissipation factor α of the junction. This had the effect of suppressing the hysteresis in the current-voltage characteristics and smearing out the fine-structure features with increasing temperature before the reduced junction length l can change much. It was possible to observe the shifts of the features of the current-voltage characteristic only in a narrow range of λ_J . In Fig. 10 the plane of the parameters (l, β) is used to demonstrate the results of perturbation theory, of numerical calculations, and of experiments on the junction No. 49.14. Numerical calculations were carried out for the transverse geometry of the junction, of the kind used in our experiments. In the calculations the values of the parameters were selected from Table I and the

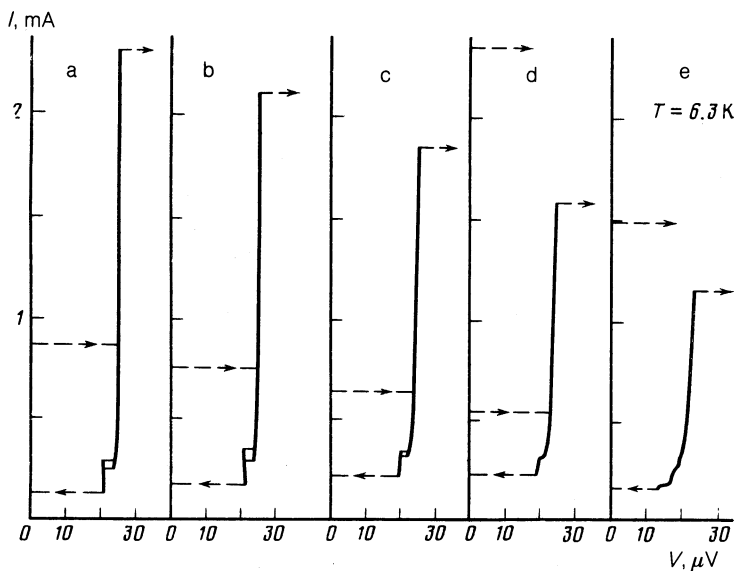


FIG. 8. Changes in the profile of the first zero-field step observed for the junction No. 49.14 with increasing temperature: a) $T = 4.2$ K; b) 4.7 K; c) 5.4 K; d) 5.9 K; e) 6.3 K (junction No. 49.14, three inhomogeneities).

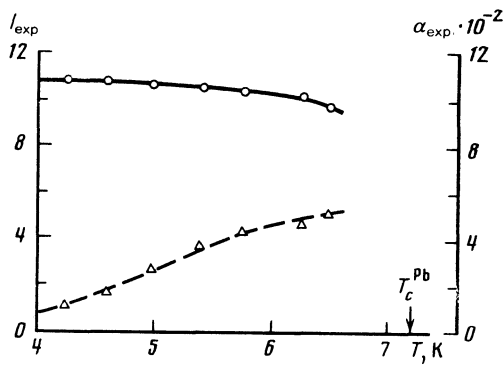


FIG. 9. Temperature dependence of the length of the junction $l = L/\lambda_j$ (O) and of the dissipation factor α (Δ) calculated from the experimental data for the junction No. 49.14.

positions of inhomogeneities corresponded to the configuration shown in Fig. 5d. An example of one of the current-voltage characteristics calculated in this way is shown in Fig. 11. When temperature was increased, the hysteresis in the region of fine structure of the experimental current-voltage characteristics disappeared in the range $\alpha_{\text{exp}} \gtrsim 0.05$, but the fine-structure features of the characteristics remained distinguishable even for $\alpha_{\text{exp}} \approx 0.1$. Two steps of the fine structure were observed (Fig. 8e) and their positions are shown in Fig. 10. It is clear from the latter figure that the theory and experiment agreed. A reduction in l shifted the features of the experimental current-voltage characteristics toward lower voltages, as deduced from perturbation theory and from numerical calculations. A negative differential resistance at resonances of the current-voltage characteristics predicted by numerical calculations (Figs. 1 and 11) was indeed observed experimentally. The additional branch of the first zero-field step of the junction No. 49.14 (Figs. 8a and 8b) had a clear negative slope, observed reliably after allowance for the experimental error in the determination of the voltage.

We shall conclude this section by noting that the most direct comparison of the theory and experiment would involve experimental determination of the frequency of the radiation emitted by an inhomogeneous junction in the region of the fine-structure features of the current-voltage

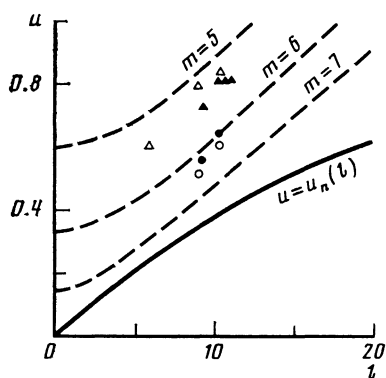


FIG. 10. Comparison of the positions of the steps on the current-voltage characteristics corresponding to soliton-plasma resonances plotted for the junction No. 49.14 on the basis of Eq. (22) (dashed curves), on the basis of numerical calculations (Δ, \circ) (for $m = 5$ and 6 , respectively) and of experimental results (\blacktriangle, \bullet); $l = 4a$.

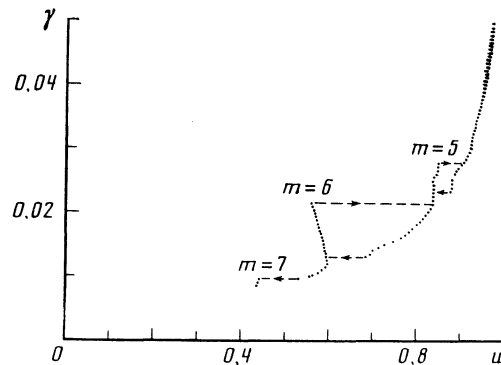


FIG. 11. Numerically calculated first zero-field step of the current-voltage characteristic of a junction with the transverse geometry and with the parameters found experimentally for the junction No. 49.14.

characteristic. Then a soliton-plasma resonance of order m should correspond to generation of the m th harmonic of the fundamental frequency in the investigated junction. However, such microwave radiation would be quite difficult to detect and this was not attempted in the present study.

7. CONCLUSIONS

Theoretical and experimental investigations were made of the motion of fluxons in Josephson junctions with regularly distributed inhomogeneities. Perturbation theory was used to obtain expressions for the harmonics of the radiation and for the decay length. The results predicted the possibility of a resonance between soliton and plasma oscillation modes and the conditions for the appearance of such a resonance were found. In the region of a resonance the current-voltage characteristic should exhibit a step of almost constant voltage. The physical mechanism responsible for such a step was assumed to be as follows: an increase of the current across the junction should result in dissipation of the supplied energy not by an increase in the velocity of a fluxon in the junction, but by an increase in the amplitude of plasma oscillations that did not contribute to the average value of the voltage across the junction. This theoretical analysis was confirmed by the results of numerical modeling of the processes in Josephson junctions with inhomogeneities. The numerically calculated current-voltage characteristics exhibited additional branches corresponding to soliton-plasma resonances.

The theoretically predicted fine-structure features of the current-voltage characteristics were observed experimentally for Nb-NbO_x-Pb junctions with deliberately formed inhomogeneities in the insulating spacer. The position of the fine-structure branches, interpreted as manifestation of soliton-plasma resonances, were in qualitative agreement with the results of perturbation theory and numerical calculations.

The observed features of the current-voltage characteristics of the junctions with deliberately formed inhomogeneities are, to the best of our knowledge, the first reliable experimental results supporting the interaction of a soliton with other types of excitations in a Josephson junction. The appearance of such features may be of interest also in applications in cryoelectronics. Soliton-plasma resonances correspond to narrow-band generation of harmonics of the fundamental frequency in a Josephson junction, which may be

useful in the generation of oscillations in the submillimeter range of wavelengths.

We are grateful to Yu. S. Gal'pern, Yu. F. Drachevskii, N. V. Zavaritskii, Yu. S. Kivshar', V. P. Koshelets, K. K. Likharev, B. A. Malomed, M. B. Mineev, I. Myugind, N. F. Pedersen, V. V. Ryazanov, A. T. Filippov, and D. E. Khmel'nitskii for valuable discussions of the results, and to N. S. Stepanov for the help in setting up the apparatus.

¹¹Radio Engineering and Electronics Institute, Academy of Sciences of the USSR, Moscow.

¹T. A. Fulton and R. C. Dynes, *Solid State Commun.* **12**, 57 (1973).

²N. F. Pedersen and D. Welner, *Phys. Rev. B* **29**, 2551 (1984).

³M. D. Fiske, *Rev. Mod. Phys.* **36**, 221 (1964).

⁴L. G. Aslamazov and E. V. Gurovich, *Pis'ma Zh. Eksp. Teor. Fiz.* **40**, 22 (1984) [*JETP Lett.* **40**, 746 (1984)].

⁵M. Cirillo, *J. Appl. Phys.* **58**, 3217 (1985).

⁶M. Cirillo, S. Pace, S. Pagano, and G. Paterno, *Phys. Lett. A* **109**, 117 (1985).

⁷Yu. S. Gal'pern and A. T. Filippov, *Zh. Eksp. Teor. Fiz.* **86**, 1527 (1984) [*Sov. Phys. JETP* **59**, 894 (1984)].

⁸A. T. Filippov, Yu. S. Galpern, T. L. Boyadiev (Boyadjiev), and I. V. Puzynin, Preprint No. E17-86-637 [in Russian], Joint Institute for Nuclear Research, Dubna (1986).

⁹D. W. McLaughlin and A. C. Scott, *Phys. Rev. A* **18**, 1652 (1978).

¹⁰G. S. Mkrtchyan and V. V. Shmidt, *Solid State Commun.* **30**, 791 (1979).

¹¹Yu. S. Kivshar and B. A. Malomed, *Phys. Lett. A* **111**, 427 (1985).

¹²K. K. Likharev, *Introduction to the Dynamics of Josephson Junctions* [in Russian], Nauka, Moscow (1985).

¹³A. Davidson, B. Dueholm, B. Kryger, and N. F. Pedersen, *Phys. Rev. Lett.* **55**, 2059 (1985).

¹⁴M. B. Mineev and V. V. Shmidt, *Zh. Eksp. Teor. Fiz.* **79**, 893 (1980) [*Sov. Phys. JETP* **52**, 453 (1980)].

¹⁵R. K. Dodd, J. C. Eilbeck, J. D. Gibbon, and H. C. Morris, *Solitons and Nonlinear Wave Equations*, Academic Press, New York (1982), p. 581.

¹⁶A. A. Golubov and A. V. Ustinov, *Pis'ma Zh. Tekh. Fiz.* **12**, 435 (1986) [*Sov. Tech. Phys. Lett.* **12**, 178 (1986)].

¹⁷A. N. Vystavkin, V. N. Gubankov, K. I. Konstantinyan, V. P. Koshelets, and Yu. V. Obukhov, *Zh. Tekh. Fiz.* **52**, 1637 (1982) [*Sov. Phys. Tech. Phys.* **27**, 1001 (1982)].

¹⁸I. L. Serpuchenko and A. V. Ustinov, *Pis'ma Zh. Eksp. Teor. Fiz.* **46**, 435 (1987) [*JETP Lett.* **46**, 549 (1987)].

Translated by A. Tybulewicz